

## NUMERICAL SIMULATION OF CONCRETE BLOCK MASONRY UNDER COMPRESSION

**Mohamad, Gihad<sup>1</sup>; Lourenço, Paulo Brandão<sup>2</sup>; Roman, Humberto Ramos<sup>3</sup>; Rizzatti, Eduardo<sup>1</sup>; Sartori, Tatiane<sup>4</sup>**

<sup>1</sup> Dr. Federal University of Santa Maria, Civil Engineering Department, [gihad.civil@gmail.com](mailto:gihad.civil@gmail.com); [edu\\_rizzatti@yahoo.com.br](mailto:edu_rizzatti@yahoo.com.br);

<sup>2</sup> PhD, Professor, University of Minho, Civil Engineering Department, [pbl@civil.uminho.pt](mailto:pbl@civil.uminho.pt)

<sup>3</sup> PhD, Professor, Federal University of Santa Catarina, Civil Engineering Department, [humberto@ecv.ufsc.br](mailto:humberto@ecv.ufsc.br)

<sup>4</sup> Federal University of Santa Maria, Master Science Student on Production Engineering Department, [tatianesartori@yahoo.com.br](mailto:tatianesartori@yahoo.com.br)

The main goal of this work is evaluate numerical model to reproduce the compression test of concrete block prisms, through a constitutive model of materials using the theory of plasticity and compare its results with experimental tests to preview the stress, strain and failure mode of the masonry. The post peak behavior of the material under tensile followed an exponential law and, under compression, a parabolic criterion was specified for the ascendant and descendent parts of the stress diagram and the hardening parameter. The mortar was connected to the block by the interface, for which the discrete model was employed, where the cracking occurred when the normal stress exceeded the tensile strength of the material.

**Keywords:** *Non-linear Behavior, Concrete Block Masonry, Interface Elements;*

### INTRODUCTION

The main deformation modes of an interface are related to kinematic phenomena, such as: localized deformation, sliding, opening and dilatance. Therefore, studies of failure mechanisms of masonry under loading are required, considering a cohesive interface (before the strength peak) and a single friction model (post peak). Martins (2001) carried out shear tests on hollow concrete block prisms with two levels of strength for the block and three for the bedding mortar. The concrete block prisms have a space between the middle blocks so that, during the tests, the blocks could slide and cause shearing at the contact between the mortar and the block. Figure 1 shows the prisms and the set up of the tests.

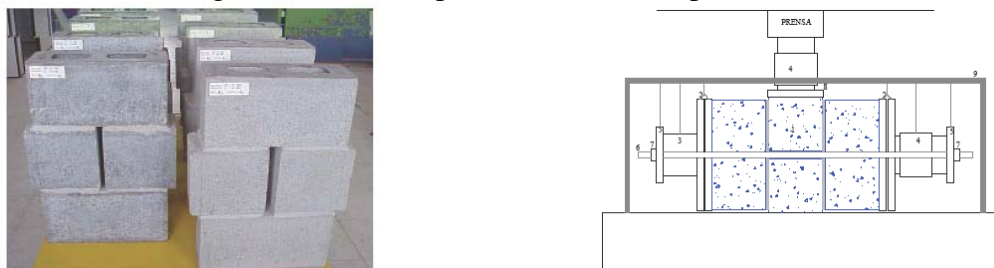


**Figure 1: Block prisms for the shear tests with and without lateral by Martins (2001).**

Abdou et. al. (2004) carried out studies on two block prisms, whose the main goal was to investigate the behavior of bedding mortar under shear stress. The nonlinearities observed in experimental tests were reproduced using an interface model. Two types of blocks (solid and hollow) were tested with the same mortar and equipment was modified to allow the experimental tests. Cycles of loading and unloading were done to obtain the displacements at the interface between brick and mortar (elastic, elastic-plastic). These cycles allowed to determine the decrease on stiffness of materials and to verify the relation between vertical and shear stress increasing, as well as, the interface behavior changing of brick and mortar under test. The authors state that the failure mode of the masonry could occur in brick (distributed cracks), in mortar (crushing) or at the interface between these materials. At the brick and mortar interface two failure modes are possible: failure by tensile (induces an opening of the joint) and shearing (sliding between the surfaces with friction). The values obtained in the experimental tests are presented in Table 1.

**Table 1: Proprieties of hollow and solid blocks.**

Brick	Proprieties	Ultimate Values
Solid	Cohesion (MPa)	c=1.58
	Friction Angle	tan (φ)=1.01
Hollow	Cohesion (MPa)	c=1.27
	Friction Angle	tan (φ)=1.01

Giambanco and Gati (1997) developed a model for cohesive interface of masonry blocks. This surface is bilinear, following *Coulomb Law* and has a tensile stress as a limit. The limit functions on stress space are presented in equations (1) and (2). Where  $\varphi$  is the internal friction angle of the material,  $s(\beta)$  and  $c(\beta)$  are the values of tensile strength and cohesion, and  $\beta$  is an internal variable which quantifies the inelastic behavior.

$$\phi_1(\sigma, \beta) = |\tau_n| + \sigma_n \cdot \tan \varphi - c(\beta) = 0 \quad (1)$$

$$\phi_2(\sigma, \beta) = \sigma_n - s(\beta) = 0 \quad (2)$$

## SIMULATION OF NON LINEAR BEHAVIOR OF PRISMS

The aim of this study is obtain a model to be able to simulate numerically the prism under compression, using a theory of plasticity as constitutive model. Figure 2 shows a diagram of a quadrangular mesh of elements with eight nodes, submitted to a plane state of stress, displacement restrictions and loadings used in the numerical model.

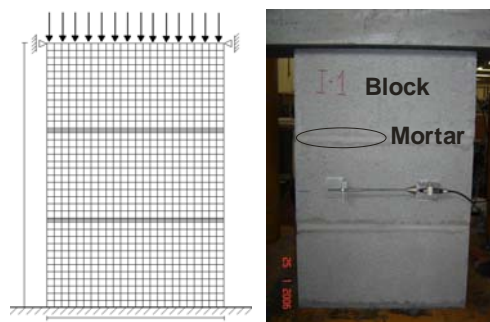


**Figure 2: Geometrical proprieties of the block and mortar set.**

The linear and nonlinear mechanical proprieties of materials in numerical simulation are presented in Table 2 and Table 3. Two mortar mixes were used in experimental tests, namely mortar type I and II. A third type of mortar designed as III were tested and we didn't observed difference in the strength and failure mode of the prisms and it wasn't presented here. The mortar proprieties of two mixes were setting in numerical simulations. The mechanical properties of mortars I and II were established considering the triaxial stress state using as a reference the compression envelope of strength, confined elasticity modulus ( $E_c$ ) and Poisson ratio ( $\nu$ ) obtained from studies of Mohamad (2007).

**Table 2: Linear mechanical characteristics of the materials.**

Component	$E_c$ (MPa)	$\nu$	$k_n$ (MPa/mm)	$k_s$ (MPa/mm)
Block	16000	0.19	-	-
Mortar - I	18000	0.10	-	-
Mortar - II	14250	0.10	-	-
Interface	-	-	81	33

**Table 3: Non linear mechanical characteristics of the materials.**

Component	c (MPa)	$f_t$ (MPa)	$\sin \varphi$	$\sin \psi$	$Gf_t$ (N/mm)	$Gf_c$ (N/mm)
Block	6.5	2.13	0.15	0.0871	0.094	12
Mortar - I	7.2	2.4	0.15	0.0871	0.094	13
Mortar - II	5.2	2.0	0.15	0.0871	0.080	11
Interface	-	2.1	-	-	-	-

## NUMERICAL RESULTS - EXPERIMENTAL RESULTS FOR TYPE A PRISMS

The main objective of the simulation was evaluated the axial and lateral strains prisms built with different mortar mix. The values of the elasticity modulus and Poisson ratio of mortar given in Table 2 used in numerical simulation consider the increase in the axial and lateral stiffness due to confinement. For prisms built with mortar I and II, it was verified that the axial stiffness obtained on numerical model was lower compared with experimental tests. Regarding the lateral strain, the numerical model managed to represent the experimental tests up to the opening of the first crack. Figures 3, 4, 5 and 6 shows a comparison between the axial and lateral stress and strain diagram of prisms obtained experimentally tests for two mortars joint (I, II) and compared with numerically results obtained at the same stress level. The results of the ultimate tensile strain of prisms were unrelated to tensile strength of block.

The appearance of localized stress at a height half of prism with mortar I induced cracks in the block, leading to an instantaneous increase in the lateral strain of the prism, as can be seen in Figures 3 and 4. Thus, the prisms constructed with mortar I did not manage to represent the lateral deformations, for stress levels above  $0.6 f_c$  (compressive strength), but a good agreement for the stress at failure point was obtained.

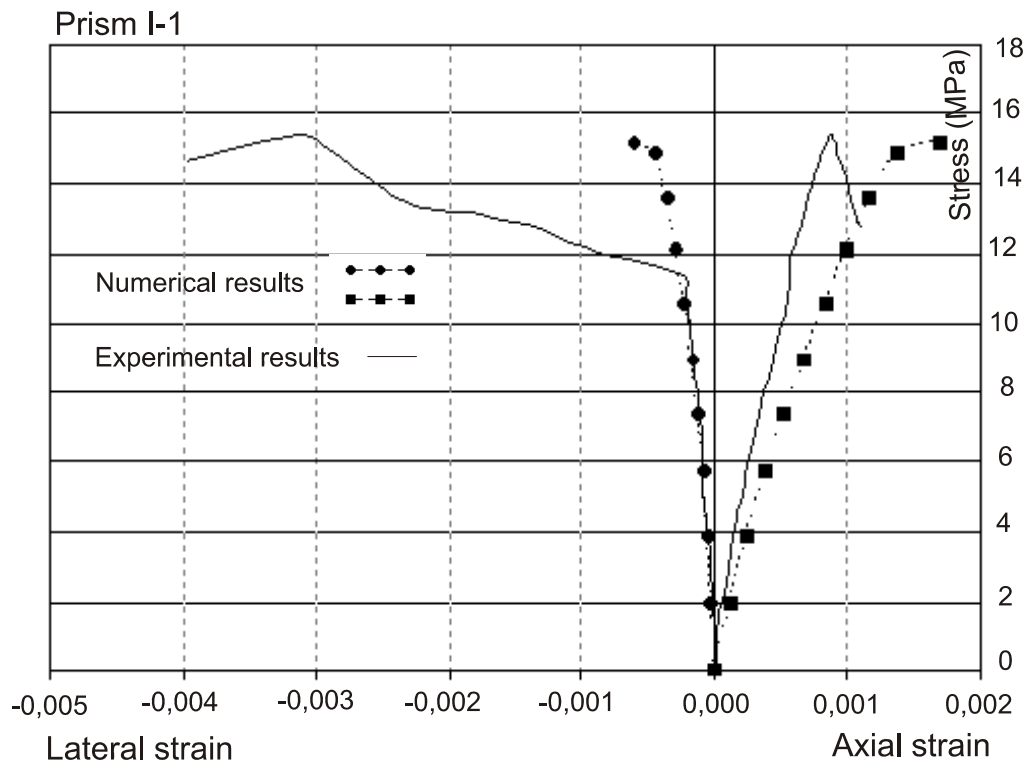


Figure 3: Axial and lateral stress and strain diagram of the prisms with mix I.

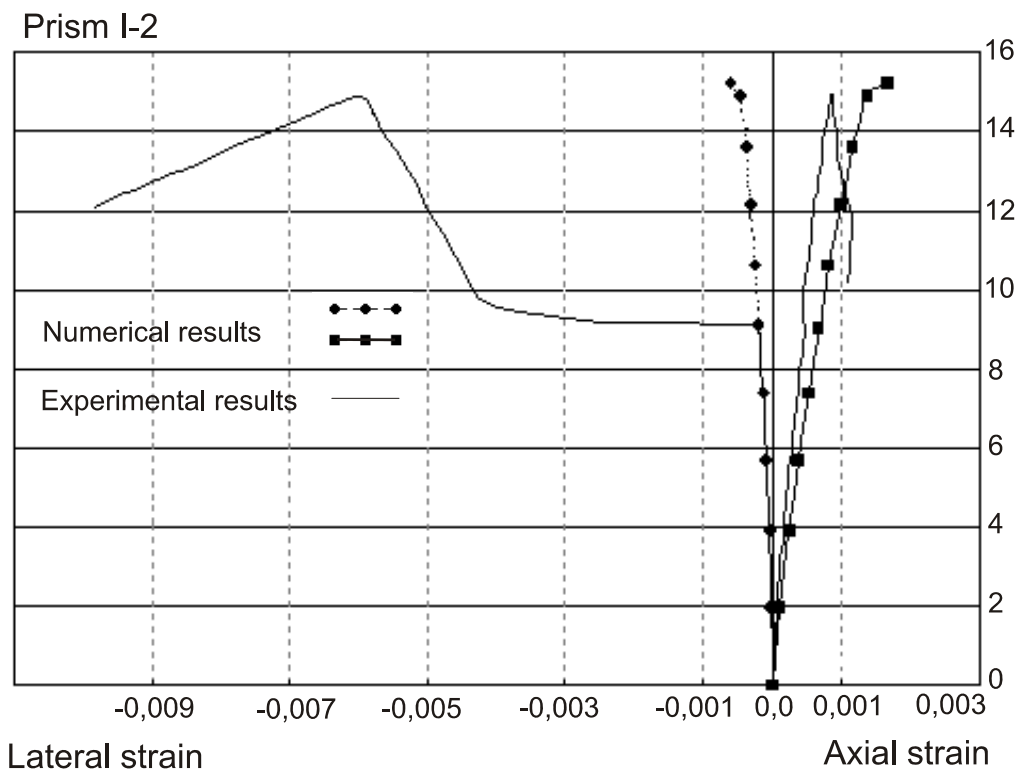
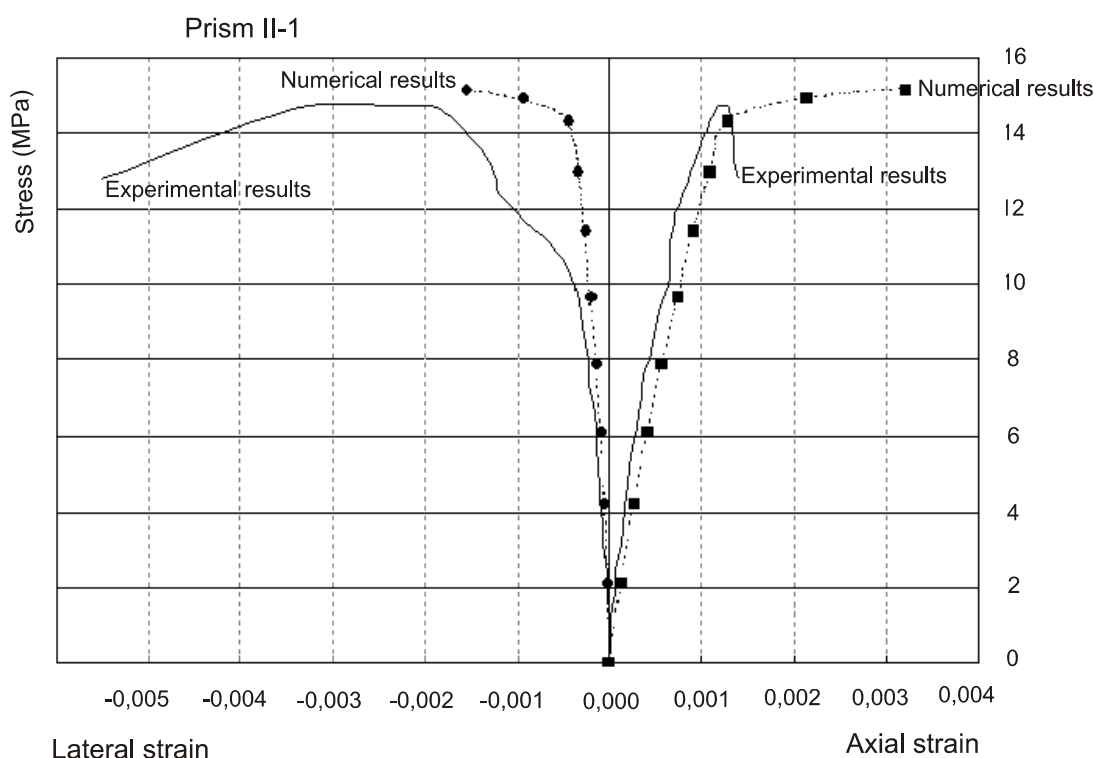


Figure 4: Axial and lateral stress and strain curves of the prisms with mix I.

The approximation between numerical and experimental results for axial and lateral strain and stress at failure point for prisms build with mortar II was better than those prisms built with mortar I. At experimental tests it was observed that the failure mode of prisms with mortar II began with the crushing of mortar. It was not observed sudden cracks opening at height half of prism. Thus, there was better agreement between the lateral and axial stresses and strain at the failure point. Table 4 shows the comparative results for the ultimate axial strain obtained in the experimental tests compared with numerical simulations. The ultimate strain is taken at the loss in the capacity of load of prisms and not for the first appearance of crack. Note that there is a significant difference in the ultimate axial strain, when the numerical and experimental results are compared for prisms I-1, I-2 and II-1, II-2.

**Table 4: Non linear mechanical characteristics of the materials.**

Prism	$\epsilon_{\text{axial ultimate}}$ (Experimental)	$\epsilon_{\text{axial ultimate}}$ (Numerical)
I-1	0.00088	0.00168
I-2	0.00086	0.00168
II-1	0.00124	0.00321
II-2	0.00332	0.00321



**Figure 5: Axial and lateral stress and strain diagram for prisms with mix II-1.**

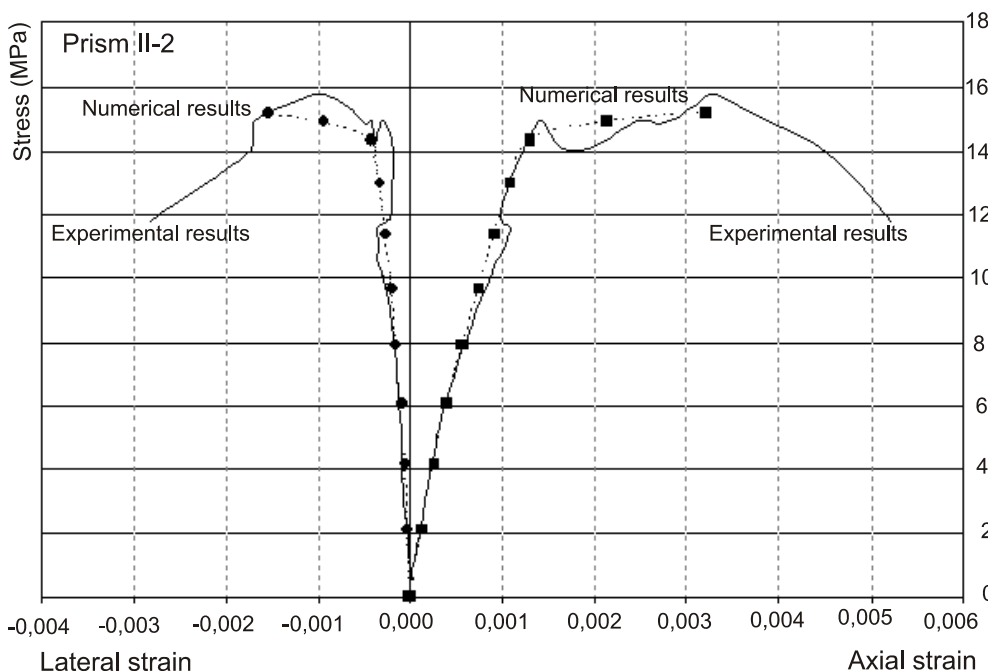


**Figure 6: Axial and lateral stress and strain diagram for prisms with mix II-2.**

The interface effect between materials (block and mortar) on the axial and lateral stress and strain values was simulated for mortar type I and II. The main conclusion of the simulation was that, under compression, it isn't possible to verify the influence of the interface between materials on the numerical results. One interpretation for this was that the interface is being constrained between blocks and the effects will be minimized by the acting force of compression. Table 5 presents the Poisson ratio results of prisms for different stress/strength ratios obtained using numerical models for mortar mixes I and II. It could be concluded from the results that there was an increase in the Poisson ratio from 0.19 to 0.36 for prisms built with bedding mortar I and 0.19 to 0.48 for prisms built with bedding mortar II.

**Table 4: Experimental results for the Poisson ratio of the prisms.**

	Mortar I	Mortar II
$\sigma/f_c$	Poisson ratio	
0	0	0
0.13	0.19	0.19
0.26	0.19	0.19
0.38	0.21	0.22
0.49	0.24	0.24
0.59	0.26	0.27
0.70	0.27	0.28
0.80	0.29	0.30
0.90	0.30	0.33
0.98	0.32	0.43
1.00	0.36	0.48

The level of vertical and horizontal stress on mortar and block were obtained on the numerical models results. The figures 7 and 8 depicted numerical results of stress on prisms for a specific element on the mortar and block. It was observed that the stress level of mortar was compression and for the block was tensile. The level of confinement stress ultimate for mortar reached 2.19 MPa and for block reached tensile stresses level ultimate of 0.12 MPa. From the results it was observed an increasing of the confinement stress during the load up to  $\sigma/f_c$  ratio close to 0.9.

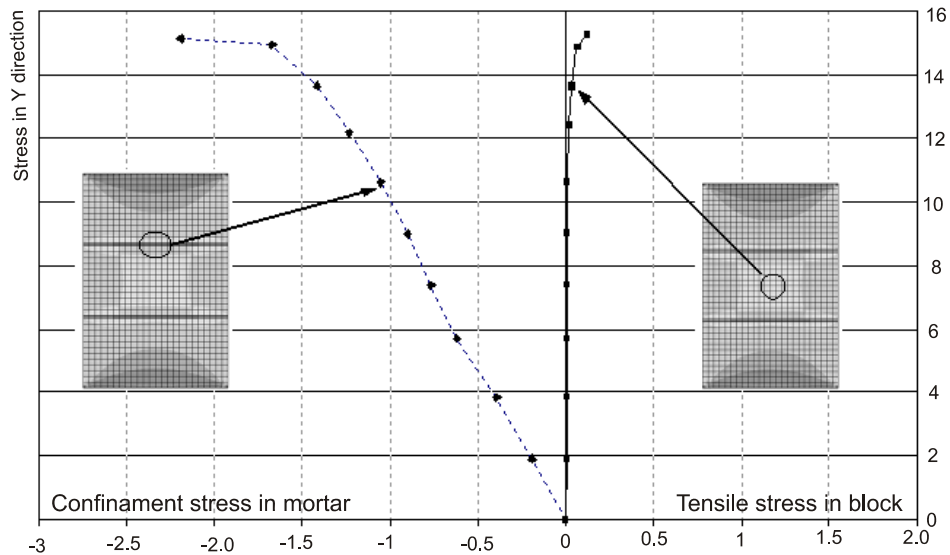


**Figure 7: Numerical stress on block and mortar I on Y direction.**

The level of confinement stress ultimate for prisms II reached 5.9 MPa on mortar and on block reached tensile stresses level ultimate of 0.37 MPa. From the results it was observed an linear increasing of the confinement stress during the load up to  $\sigma/f_c$  ratio close to 0.6. Thus, it was possible to observed the strong non linear behaviour of prisms built with mortar II, indicated that the failure mode occurs by crushing of mortar.

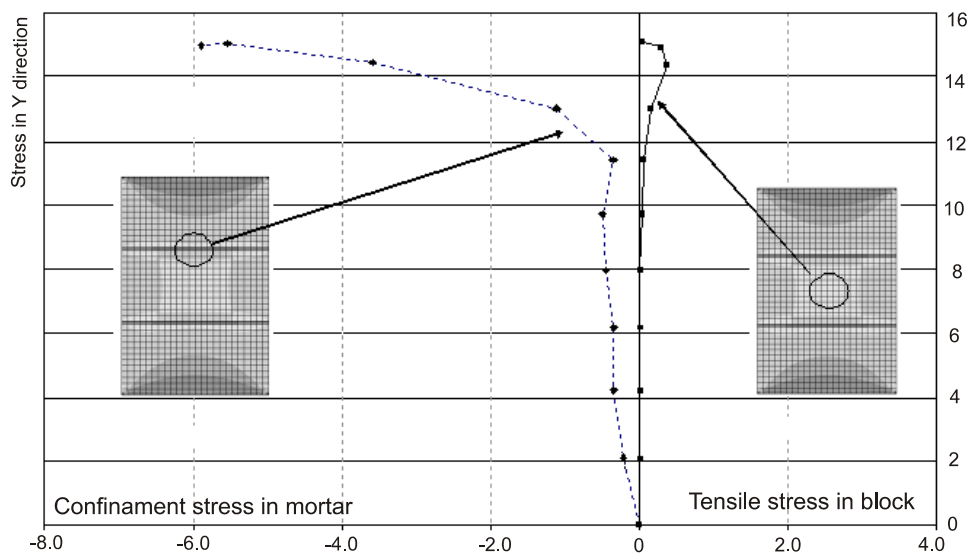


**Figure 8: Numerical stress on block and mortar II on Y direction.**



From numerical results it was possible to conclude that the level of tensile stress acting in the block was not enough to generate tensile stress that leads failure on the block, which confirms that the representation of the collapse of the materials was essentially phenomenological, requiring more advanced models to properly represent the failure of masonry. For a given element chose from numerical simulation (bedding mortar and block), it was possible to obtain a relation between the stresses and the axial and lateral strain. With these results it is possible to calculate the secant elasticity modulus until failure ( $\sigma/f_c=1$ ) was determined and depicted in the Figure 9. The upper and lower limits depicted in Figure 9 set an area which represents the behavior of the stiffness between materials. The upper limits of elasticity modulus ratio of Figure 9 reach 1,10 near failure indicating that tensile stress was developed on mortar. The lower limits of elasticity modulus ratio reach 0,85 near failure indicating that the mortar increase their stiffness with the loading and then collapsed, because of crushing of the mortar. In Figure 9 it is possible to verify that the failure modes of the prisms were differentiated, that is, for the prism-I there was a progressive increasing in the strain in  $x$  direction, producing stresses which lead to the material failure by tensile. For prism-II, there was a greater strain of the bedding joint and the failure mode occur by localized crushing on mortar and the subsequent development of tensile stresses in the block.

The Figure 10 presents the strain at failure in  $x$  direction. In the numerical simulation model it was considering the presence or not of the interface between the block and the mortar.

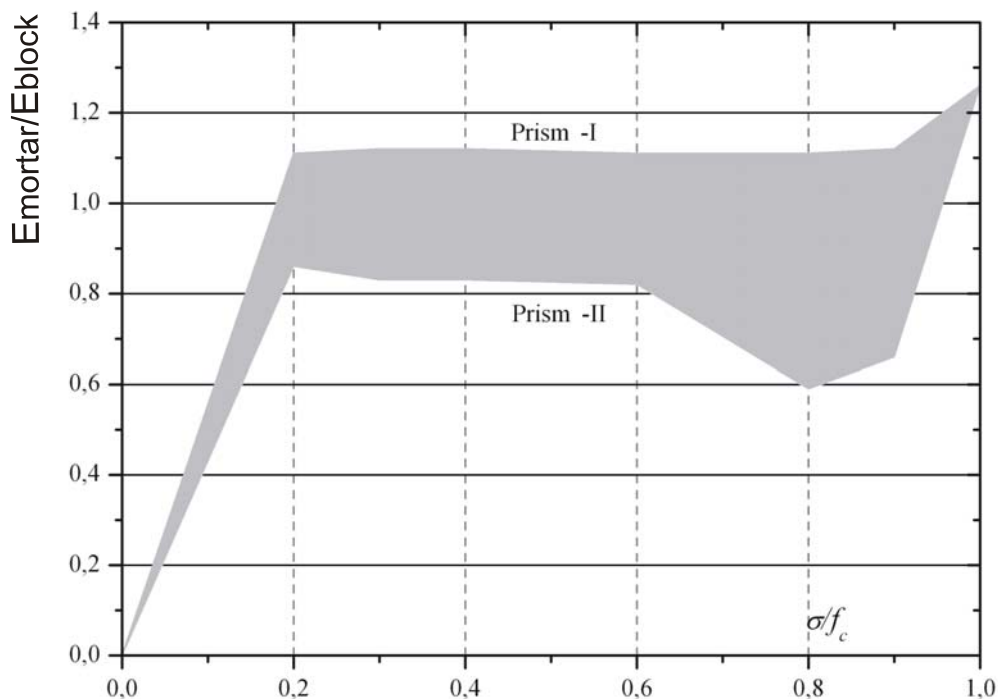


**Figure 9: Relation between  $E_{mortar}/E_{block}$  and  $\sigma/f_c$  ratio.**



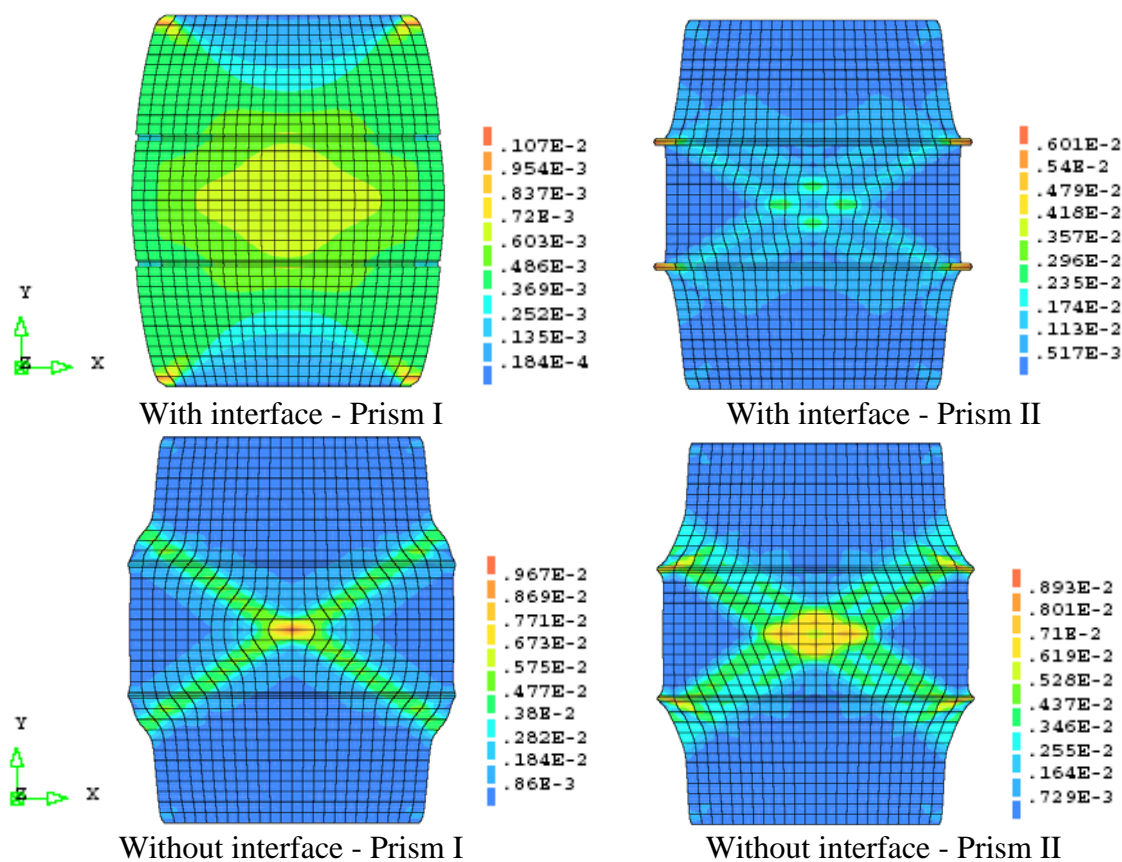


**Figure 10: Strain of prisms at  $\varepsilon_x$  directions.**

## CONCLUSIONS

The main conclusions of this work are:

- The stress and strain behaviour of prisms built with mortar type I was able to represent the axial and lateral strain until stress levels of  $0.60.f_c$ . The numerical simulation could be able to preview the failure point of the assembly. For the prisms built with mortar type II, there was a better approximation between numerical and experimental results;
- It was noted, for the three block prisms, that the effects of considering the block and mortar interface weren't significant on the strains results.
- Prisms built with mortar type I showed the development of tensile stresses in the mortar, due to an increase in its stiffness and, consequently, compression stresses were generated in the block.
- Prism built with mortar type II showed that the block was submitted to tensile stresses during the loading and the mortar to triaxial compression.
- The failure modes of the prisms were differentiated, that is, for prisms built with mortar type I there was a progressive increasing in the strain in  $x$  direction, producing stress which induced tensile on the block. The failure mode of prisms built with mortar type II was crushing of the bedding joint and then tensile stresses in the block arisen.

## REFERENCES

Martins, H. F.(2001). "Resistência ao Cisalhamento de Alvenaria estrutural de Blocos de Concreto". *Dissertação de mestrado*. Dep. de Eng. Civil. Universidade Federal de Santa

Catarina, Brasil, 2001.

Abdou, L.; Saada, R. A., Meftah, F. and Mebarki, A. (2004). “On the sliding behavior of the brick-mortar interface: An experimental study”. *Masonry International, Journal of the British Masonry Society*, 17(no 3):129-134, Winter.

Giambanco, G. and Di Gati L. (1997). “A cohesive interface model for the structural mechanics of block masonry”. *Mechanics Research*. Vol. 24(no 5), 503-512.

Atkinson, R. H.; Noland, J. L., Abrams, D. P. and McNary S. (1985). “A deformation failure theory for stack-bond brick masonry prisms in compression”. *Proc. 3rd North America Masonry Conference*, Boulder, Col.,TMS, Paper 18.

Atkinson, R. H.; Noland, J. L. and Abrams, D. P. (1985). “A deformation failure theory for stack-bond brick masonry prism in compression”. *Proceedings 7th International Brick Masonry Conference*, Melbourne, February, v.1, pp. 577-592.

Khoo, C. L. (1972). “A failure criterion for brickwork in axial compression”. *Thesis presented to University of Edinburgh*, University of Edinburgh, Scotland.

Mohamad, G. (2007). “Mecanismo de ruptura de alvenarias de blocos a compressão. *Universidade do Minho*, 312 p. Tese de Doutorado.